Ion-exosphere with anisotropic velocity distribution

by M. SCHERER (*)
Belgian Institute for Space Aeronomy
B-1180 Brussels, Belgium

Abstract. — The influence of an anisotropy in the velocity distribution at the exobase on the state variables in an open (O^+, H^+, e)-exosphere is studied for three different models corresponding respectively to an anisotropy in the velocity distribution of each species. Numerical calculations show that the effect of an anisotropy in the velocity distribution is more important for the electrons (model II) than for hydrogen ions (model I) or oxygen ions (model III). For reasonable values of the parameter characterising the anisotropy, the results do not differ qualitatively from those obtained in earlier kinetic polar wind models, i.e. the protons are accelerated outwards by a small charge separation electric field and the proton flow speed rapidly becomes supersonic.

1. INTRODUCTION

Kinetic models of the topside polar ionosphere were originally developed under the assumption that the velocity distribution at the exobase level could be approximated by a pseudo-Maxwell-Boltzmann distribution [Lemaire and Scherer, 1970, 1971]. Later on, the influence of an asymmetry in the velocity distribution function was discussed, and it was shown that the effect was negligible small for reasonable values of the parameter characterizing the asymmetry [Lemaire and Scherer, 1972]. In this paper we will study the effect of an anisotropy

(*) Présenté par M. NICOLET.

in the velocity distribution. We assume that the velocity distribution function at the exobase is given by the bi-maxwellian

$$f[r_o, \vec{v}(r_o)] = \mathrm{N}\left(\frac{m}{2\pi k \mathrm{T}_{\|}}\right)^{1/2}\left(\frac{m}{2\pi k \mathrm{T}_{\perp}}\right)\exp\left[-\frac{m}{2k\mathrm{T}_{\|}}v_{\|}^2 - \frac{m}{2k\mathrm{T}_{\perp}}v_{\perp}^2\right] \quad (1)$$

where r_o is the radial distance of the exobase, $\vec{v}(r_o)$ is the velocity vector at the exobase of a particle with mass m, $v_{\|}$ and $v_{\perp}$ are the components of $\vec{v}(r_o)$ respectively parallel and perpendicular to the magnetic field, k is the Boltzmann constant, and N, $\mathrm{T}_{\|}$ and $\mathrm{T}_{\perp}$ are three parameters which can be determined so that the calculated number density, temperature and temperature anisotropy at the exobase have given values. According to Miller [1972] and Clark *et al.* [1973] this is a more realistic form for the high-altitude thermal electrons than is an isotropic Maxwellian distribution function.

Analytical expressions for the number density, the escape flux, the parallel and perpendicular momentum fluxes, and the energy flux in the open ion-exosphere recently have been determined [Scherer, 1978] under the assumptions that (*i*) the velocity distribution at the exobase is given by (1); (*ii*) along a magnetic field line the potential energy of a charged particle is a monotonic function; and (*iii*) the magnetic field strength decreases monotonically to a constant value.

Since the magnetic field strength at the exobase is much larger than the interplanetary magnetic field, we assume in what follows that this constant is zero. It can be shown that, although this assumption simplifies the calculations, it will not modify the results and the conclusions of this study.

For particles moving in a potential well, the formulae for the state variables do not depend on the magnetic field strength at infinity. Hence they are given by [Scherer, 1978]:

(*a*) the number density:

$$n(s) = \frac{1}{2}\mathrm{N}\alpha\left[\mathrm{erfex}(\mathrm{V}_x) - b\,\mathrm{erfex}(\mathrm{V}_x/b)\right] \quad (2)$$

(*b*) the escape flux:

$$\mathrm{F}(s) = \frac{1}{2}\mathrm{N}\eta(2k\mathrm{T}_{\|}/\pi m)^{1/2} \quad (3)$$

$$P_{\perp}^{(E)}(s) = \frac{1}{2} N k T_{\perp} \alpha \left\{ \alpha \operatorname{erfex}(V_c) - M_1 b \operatorname{erfex}(X/b) \right.$$

$$\left. + \frac{2}{\sqrt{\pi}} \left[\alpha V_c + \frac{2}{3} \alpha V_c^3 - M_1 X - \frac{2t}{3\mu} \left(1 + \frac{\eta}{2} \right) X^3 \right] \right\} \exp\left[- q(\infty) \right]$$

$$\text{for } t = 1 \quad (16)$$

(d) the energy flux parallel to the magnetic field:

$$\varepsilon(s) = \frac{1}{2} N k T_{\parallel} (2k T_{\parallel}/\pi m)^{1/2} \eta \left\{ \left[1 + \frac{1 + t V_c^2}{t - 1} \right] \exp\left[- q(\infty) \right] \right.$$

$$\left. - \frac{1}{t - 1} \left[\frac{1}{t} - q(s) \right] \exp\left[- t q(\infty) \right] \right\} \qquad \text{for } t \neq 1 \quad (17)$$

$$\varepsilon(s) = \frac{1}{2} N k T_{\parallel} (2k T_{\parallel}/\pi m)^{1/2} \eta \exp\left[- q(\infty) \right]$$

$$\left\{ \left[1 + q(\infty) \right] (2 + V_c^2) - q(\infty) \right\} \cdot \qquad \text{for } t = 1 \quad (18)$$

In formulae (9) to (18) we have used the shorthand notations:

$$V_c^2 = q(\infty) - q(s) \geqslant 0; \qquad X^2 = pq(\infty) - q(s) \geqslant 0 \quad (19)$$

$$Z(x) = \begin{cases} \gamma \mathscr{D}(x/\gamma) \text{ with } \gamma^2 \equiv \eta/(t - 1) & \text{if } t > 1 \\ - \beta \operatorname{erfex}(x/\beta) \text{ with } \beta^2 \equiv \eta/(1 - t) & \text{if } t < 1 \end{cases} \quad (20)$$

$$\mathscr{D}(z) = \frac{2}{\sqrt{\pi}} \exp(- z^2) \int_0^z \exp(x^2) dx. \quad (21)$$

For the *ballistic particles* the number density and the parallel and perpendicular momentum fluxes can be determined by means of the following formulae [Scherer, 1978]

$$n^{(B)}(s) = N\alpha \left\{ \exp\left[- q(s) \right] - b \exp\left[- q(s)/b^2 \right] \right\} - 2n^{(E)}(s) \quad (22)$$

$$P_{\parallel}^{(B)}(s) = N k T_{\parallel} \alpha \left\{ \exp\left[- q(s) \right] - b^3 \exp\left[- q(s)/b^2 \right] \right\} - 2P_{\parallel}^{(E)}(s) \quad (23)$$

$$P_{\perp}^{(B)}(s) = N k T_{\perp} \alpha \left\{ \alpha \exp\left[- q(s) \right] - M_1 b \exp\left[- q(s)/b^2 \right] \right\} - 2P_{\perp}^{(E)}(s) \quad (24)$$

where $n^{(E)}(s)$, $P_{\parallel}^{(E)}(s)$, and $P_{\perp}^{(E)}(s)$ are respectively given by (9) and (10), (13) and (14), and (15) and (16).

To illustrate the influence of an anisotropy in the velocity distribution function, we consider an (O^+, H^+, e) exosphere. At the exobase, assumed to be at 1000 km above the polar cap, the relative number densities are given by

$$n_e(s_o): n_{O^+}(s_o): n_{H^+}(s_o) = 1:0.9:0.1. \tag{25}$$

Hence the quasi-neutrality condition

$$n_e = n_{O^+} + n_{H^+} \tag{26}$$

is satisfied at the exobase.

The parameters N_e, N_{O^+}, and N_{H^+} entering in the velocity distribution (1), written down for each species, can be determined by means of (25) (see appendix A). Moreover we assume that $T_{\perp,e} = T_{\perp,O^+} = T_{\perp,H^+} = 3000$ K. The influence of the anisotropy $t = T_{\parallel}/T_{\perp} \neq 1$ in the distribution (1) will be studied for three different kinds of models. In model I we assume that the velocity distribution of the electrons and oxygen ions is isotropic; i.e. $T_{\parallel,e} = T_{\perp,e}$ or $t_e = 1$ and $T_{\parallel,O^+} = T_{\perp,O^+}$ or $t_{O^+} = 1$. The velocity distribution of the hydrogen ions, however, is anisotropic ($T_{\parallel,H^+} \neq T_{\perp,H^+}$) and in Sec II some results corresponding to different values of $T_{\parallel,H^+}$ are illustrated. In model II the velocity distribution of the ions is isotropic ($t_{H^+} = t_{O^+} = 1$) and the velocity distribution of the electrons is a bi-maxwellian with $T_{\parallel,e} \neq T_{\perp,e}$. The numerical results obtained for this model are discussed in Sec. III. Finally, in Sec IV, we illustrate model III for which the velocity distributions of the electrons and hydrogen ions are isotropic ($t_e = t_{H^+} = 1$), whereas the velocity distribution of the oxygen ions is assumed to be anisotropic ($T_{\parallel,O^+} \neq T_{\perp,O^+}$). All numerical calculations are made for the magnetic dipole field along the magnetic field line intersecting the magnetic pole.

2. Influence of an anisotropy in the hydrogen velocity distribution function

Assuming that at the exobase the velocity distributions of the electrons and oxygen ions are given by a pseudo-maxwellian (i.e. $t_e = t_{O^+} = 1$ or $T_e = T_{\parallel,e} = T_{\perp,e}$ and $T_{O^+} = T_{\parallel,O^+} = T_{\perp,O^+}$), we will study the effect of an anisotropy in the velocity distribution function of the hydrogen ions. Early kinetic model calculations of the topside

polar ionosphere [Lemaire and Scherer, 1969, 1970] have shown that the electrostatic potential at the exobase can be determined by the condition

$$F_e(s_o) = F_{H^+}(s_o) + F_{O^+}(s_o) \tag{27}$$

which expresses the fact that the electron flux equals the total ion flux. Moreover it was shown that the hydrogen ions move in a potential well; i.e. all hydrogen ions are accelerated outwards by the electric force, and escape. Therefore the escape flux of the hydrogen ions can be calculated by means of formula (3) or, taking into account (A1),

$$F_{H^+}(s_o) = a_{H^+} t_{H^+}^{1/2} \tag{28}$$

with

$$a_{H^+} = (2kT_{\perp,H^+}/\pi m_{H^+})^{1/2} n_{H^+}(s_o). \tag{29}$$

The escaping electrons and oxygen ions, on the contrary, have to overcome a potential barrier and their escape flux is given by (12) which, according to (A3) and (A4), is equivalent to

$$F_j(s_o) = a_j h(Q_j)[1 + q_j(\infty)] \exp[-q_j(\infty)] \tag{30}$$

where j stands for the subscripts e and 0^+, and where we have used the shorthand notations

$$h(Q_j) = \left[1 + \operatorname{erf}(Q_j) - \frac{2}{\sqrt{\pi}} Q_j \exp\left(-Q_j^2\right)\right]^{-1} \tag{31}$$

$$Q_j = [q_j(\infty)]^{1/2}.$$

Since the hydrogen escape flux depends on t_{H^+} (the parameter characterizing the anisotropy) the heights of the reduced potential barriers $q_j(\infty)$ will also depend on t_{H^+}. Differentiation of (30) with respect to t_{H^+} yields

$$\frac{dF_j(s_o)}{dt_{H^+}} = -\alpha_j \frac{dq_j(\infty)}{dt_{H^+}} \tag{32}$$

with

$$\alpha_j = a_j Q_j h(Q_j) \exp[-q_j(\infty)] \left\{ Q_j + \frac{2}{\sqrt{\pi}} [1 + q_j(\infty)] h(Q_j) \right.$$

$$\left. \cdot \exp[-q_j(\infty)] \right\} > 0. \tag{33}$$

From the definition of $q(s)$ in (7) and (8), it follows that

$$q_j(\infty) = -(Z_j e\varphi(s_o) - Gm_j M/r_o)/kT_{\parallel,j} \tag{34}$$

and

$$\frac{dq_j(\infty)}{dt_{H^+}} = -\frac{Z_j e}{kT_{\parallel,j}} \frac{d\varphi(s_o)}{dt_{H^+}}. \tag{35}$$

Substitution of (35) in the right-hand side of (32) yields for the electrons ($Z_e = -1$)

$$\frac{dF_e(s_o)}{dt_{H^+}} = -\frac{e\alpha_e}{kT_e} \frac{d\varphi(s_o)}{dt_{H^+}} \tag{36}$$

and for the oxygen ions ($Z_{O^+} = +1$).

$$\frac{dF_{O^+}(s_o)}{dt_{H^+}} = \frac{e\alpha_{O^+}}{kT_{O^+}} \frac{d\varphi(s_o)}{dt_{H^+}}. \tag{37}$$

After differentiation of the relation (27) with respect to t_{H^+}, and taking into account (28), (36) and (37) we obtain

$$\frac{d\varphi(s_o)}{dt_{H^+}} = -\frac{k}{2e} a_{H^+} t_{H^+}^{-1/2} \Big/ \left(\frac{\alpha_e}{T_e} + \frac{\alpha_{O^+}}{T_{O^+}}\right) < 0. \tag{38}$$

This shows that the electrostatic potential at the exobase is a decreasing function of the anisotropy parameter t_{H^+}. This result is illustrated in fig. 1 (curve I). Considering (35) and (38) we can conclude that the height of the potential barrier decreases for the electrons (see fig. 2a, curve I) and increases for the oxygen ions (see fig. 2*b*, curve I), whereas for the hydrogen ions $| q_{H^+}(\infty) |$, the depth of the potential well decreases very rapidly with increasing values of t_{H^+} (see fig. 2c, curve I).

The electrostatic potential distribution in the exosphere and the deduced electric field are plotted respectively in fig. 3 and fig. 4 for three model calculations corresponding to the parameter values $t_{H^+} = 0.25$; 1, and 4. Close to the exobase the electrostatic potential is a rapidly decreasing function of altitude, and the electric field is almost independent of the t_{H^+}-values. At higher altitudes the electric field decreases with increasing values of the anisotropy. As a consequence of this the electric force acting on the thermal electrons diminishes, and therefore the escape flux of the electrons will increase. This result follows also from formulae (36) and (38). Moreover, from (37) and (38)

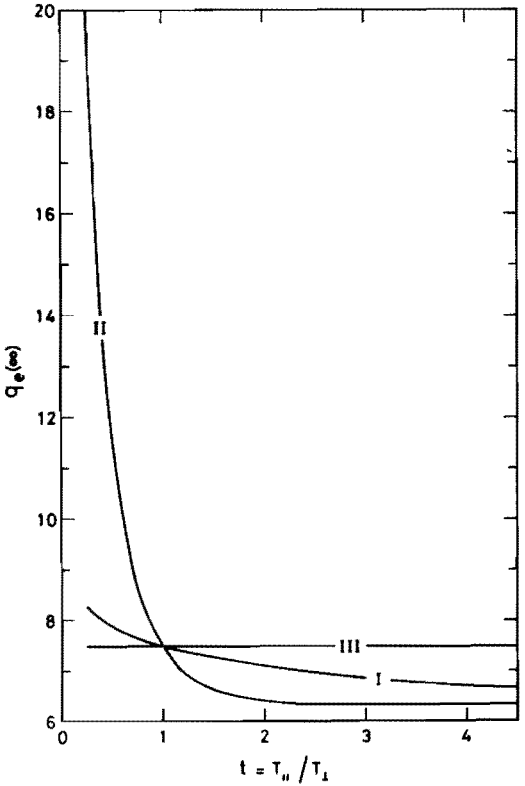

FIG. 2a. — The reduced potential barrier height for the electrons as a function of the anisotropy parameter for anisotropic velocity distributions of the hydrogen ions (curve I), electrons (curve II), and oxygen ions (curve III).

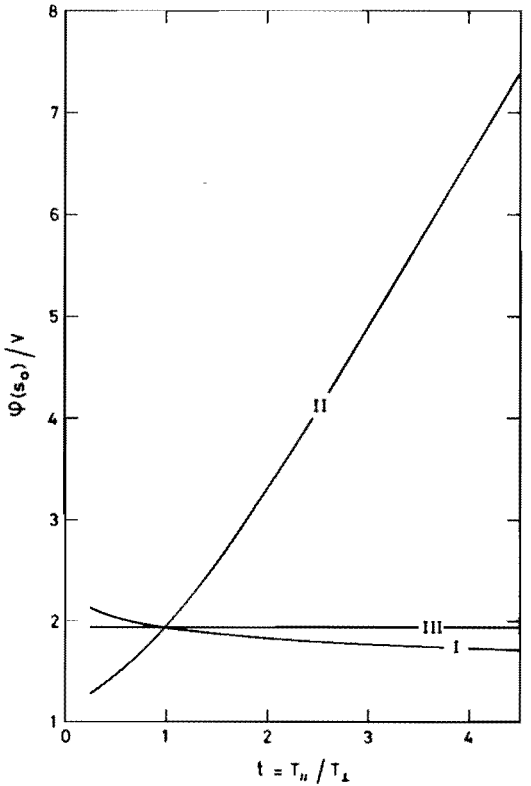

FIG. 1. — The electrostatic potential at the exobase as a function of the anisotropy parameter for anisotropic velocity distributions of the hydrogen ions (curve I), electrons (curve II) and oxygen ions (curve III).

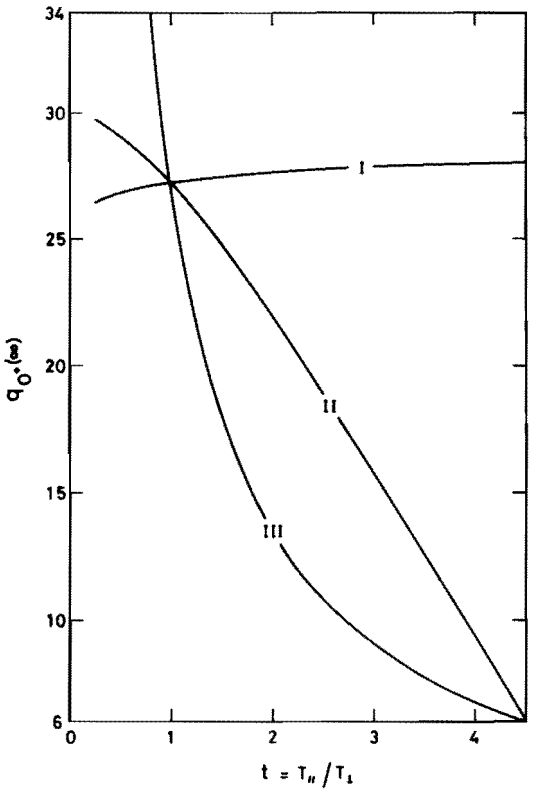

FIG. 2b. — The reduced potential barrier height for the oxygen ions as a function of the anisotropy parameter for anisotropic velocity distributions of the hydrogen ions (curve I), electrons (curve II), and oxygen ions (curve III).

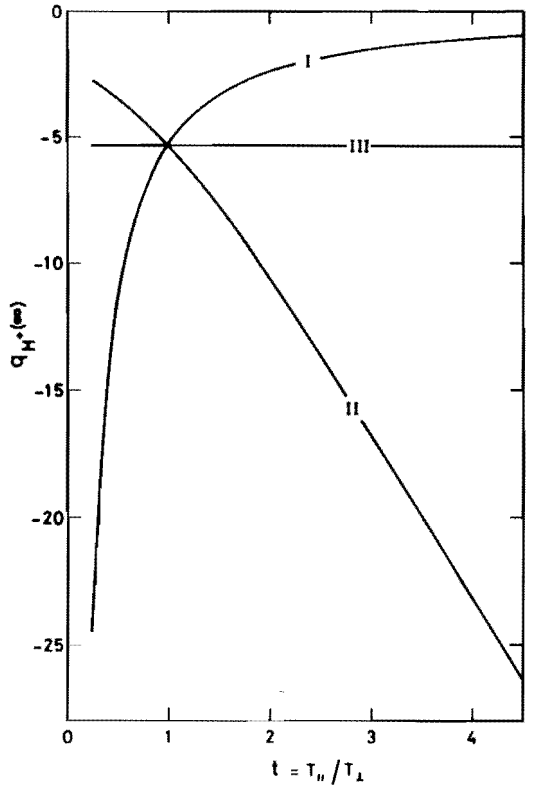

FIG. 2c. — The reduced potential well depth for the hydrogen ions as a function of the anisotropy parameter for anisotropic velocity distributions of the hydrogen ions (curve I), electrons (curve II), and oxygen ions (curve III).

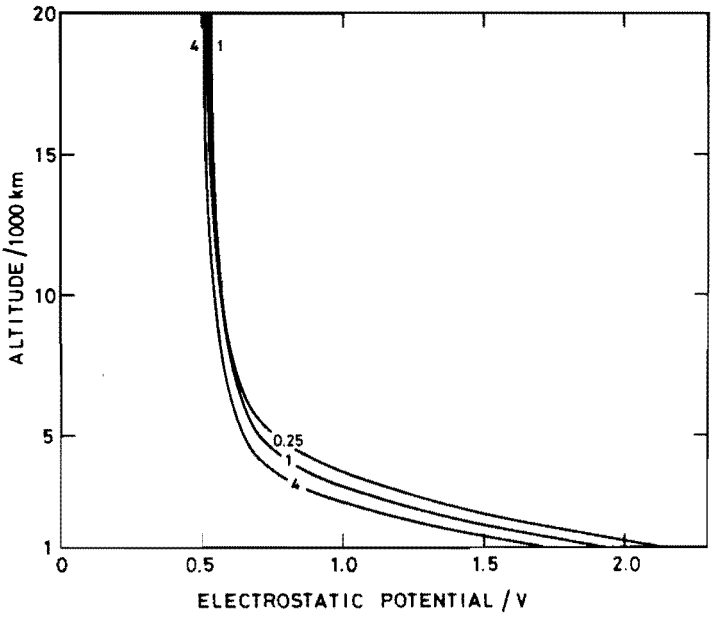

FIG. 3. — The electrostatic potential distribution in the exosphere for three different hydrogen ion velocity distributions corresponding respectively to the anisotropy parameter values $t_{H+} = 0.25; 1; 4$.

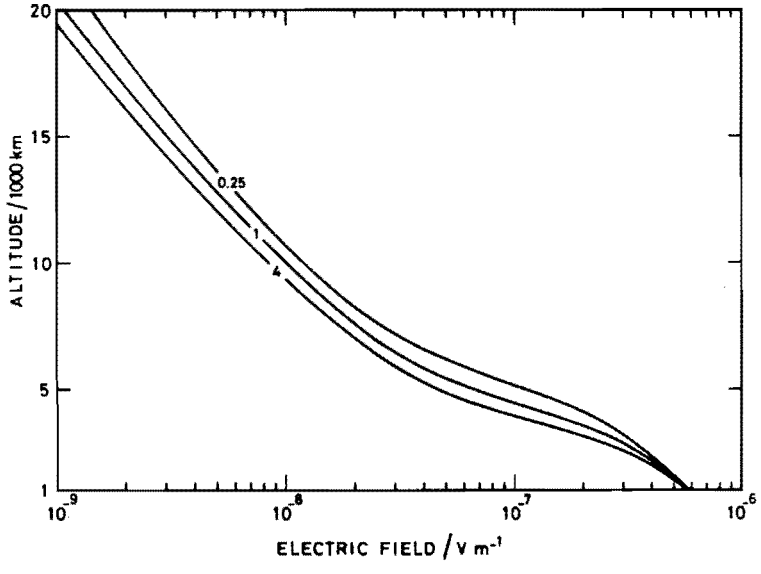

FIG. 4. — The electrostatic electric field distribution in the exosphere for three different hydrogen ion velocity distributions corresponding respectively to the anisotropy parameter values $t_{H+} = 0.25; 1; 4$.

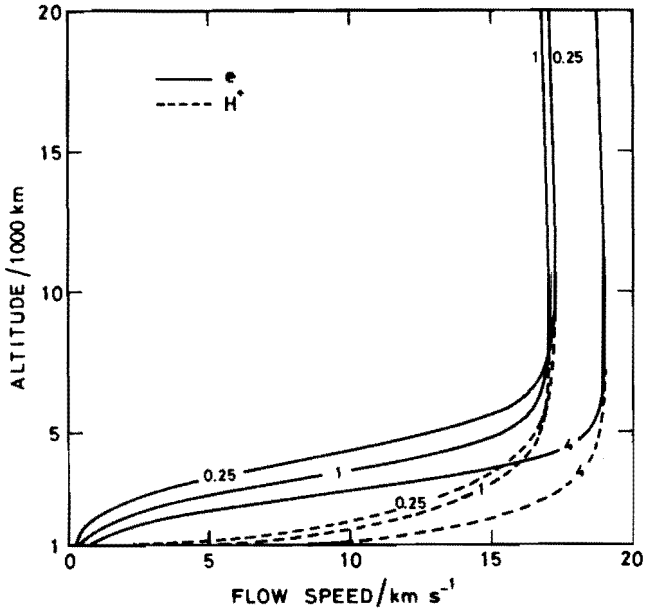

FIG. 5. — The electron and hydrogen ion flow speed in the exosphere for three different hydrogen ion velocity distributions corresponding respectively to the anisotropy parameter values $t_{H^+} = 0.25; 1; 4$.

we can deduce that the escape flux of the oxygen ions decreases for increasing values of t_{H^+}, so that the electron escape flux is almost completly balanced by the hydrogen efflux. Finally, the influence of an anisotropy in the hydrogen-ion velocity distribution on the flow speeds of the electrons and hydrogen ions is illustrated in fig. 5 where the flow speed is defined by

$$w_j(s) = F_j(s)/n_j(s) \tag{39}$$

the subscript j standing for e and H^+.

3. INFLUENCE OF AN ANISOTROPY IN THE ELECTRON VELOCITY DISTRIBUTION FUNCTION

In what follows we assume that the velocity distribution of the ions is given by a pseudo-maxwellian (i.e. $t_{H^+} = t_{O^+} = 1$, or $T_{H^+} = T_{\parallel,H^+} = T_{\perp,H^+}$ and $T_{O^+} = T_{\parallel,O^+} = T_{\perp,O^+}$) and we will study the effect of

an anisotropy in the velocity distribution of the electrons. The escape flux of the hydrogen ions is given by (28) where $t_{H^+} = 1$, and the oxygen ion escape flux is still defined by (30). Hence

$$\frac{dF_{H^+}(s_o)}{dt_e} = 0 \tag{40}$$

$$\frac{dF_{O^+}(s_o)}{dt_e} = \frac{eZ_{O^+}\alpha_{O^+}}{kT_{O^+}} \frac{d\varphi(s_o)}{dt_e} \tag{41}$$

where α_{o^+} is defined by (33).

The escape flux of the electrons is now given by (11) which, taking into account (A3) and (A4), is equivalent to

$$F_e(s_o) = a_e t_e^{1/2} A[t_e, q_e(\infty)]/B(Q_e) \tag{42}$$

with

$$A[t_e, q_e(\infty)] = \{t_e \exp[-q_e(\infty)] - \exp[-t_e q_e(\infty)]\}/(t_e - 1) \tag{43}$$

$$B(Q_e) = 1 + \operatorname{erf}(Q_e) - S(Q_e) \tag{44}$$

and where $S(Q_e)$ is defined in (A4).

Differentiation of (34), (43) and (44) yields

$$t_e \frac{dq_e(\infty)}{dt_e} = -q_e(\infty) - \frac{eZ_e}{kT_{\perp,e}} \frac{d\varphi(s_o)}{dt_e} \tag{45}$$

$$\frac{dA[t_e, q_e(\infty)]}{dt_e} = \beta_e - \gamma_e \frac{d\varphi(s_o)}{dt_e} \tag{46}$$

with

$$\beta_e = \{1 - [1 - (t_e - 1)q_e(\infty)] \exp[(t_e - 1)q_e(\infty)]\}$$
$$\cdot (t_e - 1)^{-2} \exp[-t_e q_e(\infty)] > 0 \tag{47}$$

$$\gamma_e = \frac{eZ_e}{kT_{\perp,e}} \{\exp[-t_e q_e(\infty)] - \exp[-q_e(\infty)]\}/(t_e - 1) > 0 \tag{48}$$

$$\frac{dB(Q_e)}{dt_e} = \lambda_e \frac{d\varphi(s_o)}{dt_e} - \mu_e \tag{49}$$

with

$$\lambda_e = -\frac{eZ_e}{kT_{\perp,e}} S(Q_e) > 0 \tag{50}$$

$$\mu_e = \frac{1}{2}\left\{\frac{2}{\sqrt{\pi}} Q_e \exp[-Q_e^2] - S(Q_e)\right\} \Big/ (t - 1) > 0. \tag{51}$$

It can easily be shown that the functions β_e, γ_e, λ_e and μ_e are positive. Calculating the derivative of the escape flux $F_e(s_o)$ with respect to t_e, and taking into account the results (46) and (49) yields

$$\frac{dF_e(s_o)}{dt_e} = \tau_e - v_e \frac{d\varphi(s_o)}{dt_e} \tag{52}$$

with

$$\tau_e = a_e t_e^{1/2} \left\{ \beta_e + \left[\frac{1}{2t_e} + \mu_e / B(Q_e) \right] A[t_e, q_e(\infty)] \right\} \Big/ B(Q_e) > 0 \tag{53}$$

$$v_e = a_e t_e^{1/2} \{ \gamma_e + \lambda_e A[t_e, q_e(\infty)] / B(Q_e) \} / B(Q_e) > 0. \tag{54}$$

From the zero flux condition (27) and the results (40), (41) and (52) the following relation is deduced:

$$\frac{d\varphi(s_o)}{dt_e} = \tau_e \left[v_e + eZ_{O^+} \alpha_{O^+} / kT_{O^+} \right]^{-1} > 0. \tag{55}$$

Hence, the electrostatic potential at the exobase will increase with the electron anisotropy parameter t_e. This is in accordance with the numerical results plotted in fig. 1, curve II.

Substitution of (55) in (52) gives

$$\frac{dF_e(s_o)}{dt_e} = eZ_{O^+} \alpha_{O^+} \tau_e \left[v_e kT_{O^+} + eZ_{O^+} \alpha_{O^+} \right]^{-1} > 0 \tag{56}$$

which shows that the electron escape flux increases with t_e. On the other hand it can be shown from (34) that

$$\frac{dq_j(\infty)}{dt_e} = -\frac{e}{kT_{\|,j}} \frac{d\varphi(s_o)}{dt_e} < 0 \tag{57}$$

where the subscript j stands for O^+ and H^+. From (57) it can be concluded that the height of the potential barrier that the escaping oxygen ions have to overcome, will decrease with an increasing anisotropy t_e (see fig. 2*b*, curve II). As a consequence of this the oxygen escape flux $F_{O^+}(s_o)$ will increase in order to balance the enhanced electron escape flux, the hydrogen ion escape flux $F_{H^+}(s_o)$ being constant. From (55) it can be deduced also that $| q_{H^+}(\infty) |$, the depth of the potential well of the hydrogen ions, increases with t_e. This is illustrated in fig. 2c, curve II. The height of the potential barrier of the electrons decreases very strongly in the interval $t_e \leqq 1$, for larger values of the parameter t_e the decrease of $q_e(\infty)$ is much less (see fig. 2a, curve II).

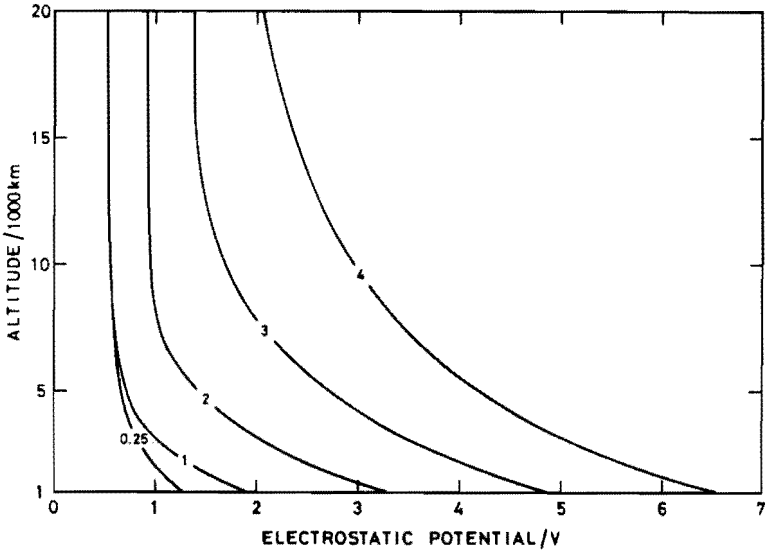

FIG. 6. — The electrostatic potential distribution in the exosphere for five different electron velocity distributions corresponding respectively to the anisotropy parameters values $t_e = 0.25; 1; 2; 3; 4$.

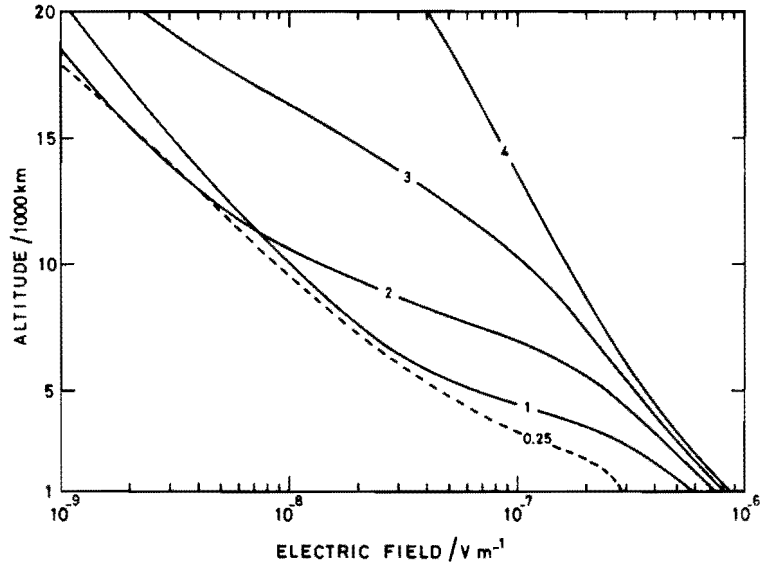

FIG. 7. — The electrostatic electric field distribution in the exosphere for five different electron velocity distributions corresponding respectively to the anisotropy parameter values $t_e = 0.25; 1; 2; 3; 4$.

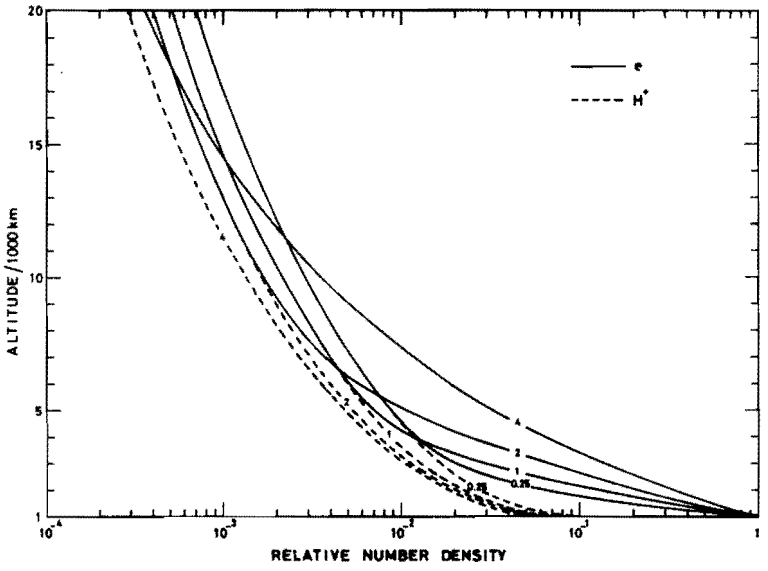

FIG. 8a. — The relative number densities of the electrons and hydrogen ions in the exosphere for five different electron velocity distributions corresponding respectively to the anisotropy parameter values $t_e = 0.25; 1; 2; 3; 4$.

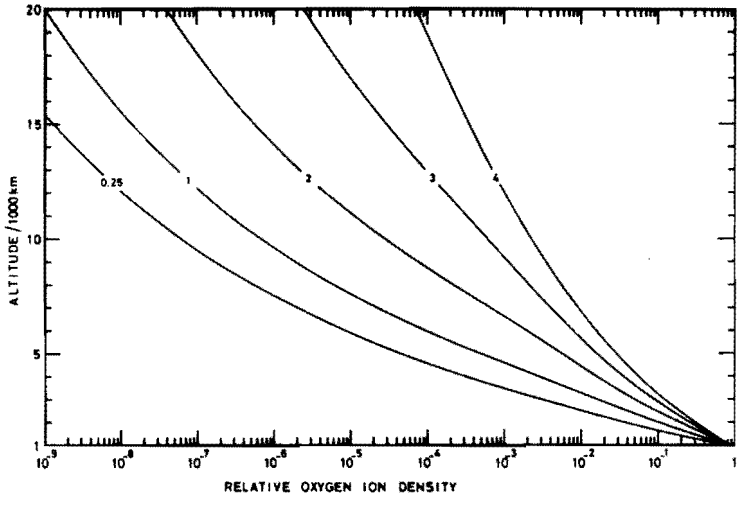

FIG. 8b. — The relative oxygen ion number density in the exosphere for five different electron velocity distributions corresponding respectively to the anisotropy parameter values $t_e = 0.25; 1; 2; 3; 4$.

The electrostatic potential distribution and the deduced electric field in the exosphere are plotted respectively in fig. 6 and fig. 7 for five model calculations corresponding to the values $t_e = 0.25$; 1; 2; 3 and 4. Although the electrostatic potential increases with t_e, the general behaviour is not influenced; near the exobase, $\varphi(s)$ is a rapidly decreasing function of altitude which tends asymptotically to zero at greater distances. The electric field decreases with altitude for the five models illustrated in fig. 7.

The relative number densities of the electrons and hydrogen ions are plotted in fig. 8a. The larger values of t_e correspond to the smaller values of the hydrogen ion density. This is also true for the electron concentration at higher altitudes. Near the exobase, however, the electron number density distribution is an increasing function of t_e. The altitude for which the oxygen ion density becomes negligible small as compared with the hydrogen ion density (i.e. the altitude for which $n_e(s) \cong n_{H^+}(s)$) depends very strongly on the t_e-value. For $t_e = 0.25$ this happens at about 4500 km; for $t_e = 1$ at 6500 km, for $t_e = 2$ at 10.000 km and for $t_e = 4$ above 20.000 km. Since for the extreme values of t_e considered here (i.e. 0.25 and 4) the electron density changes by less than one order of magnitude, it can be concluded that the oxygen ion density decreases much less rapidly with altitude for larger t_e values. This is illustrated in fig. 8b, which shows that at 5000 km the oxygen ion density is two orders of magnitude larger for $t_e = 4$ as compared with the corresponding value for $t_e = 1$. At 20.000 km altitude there is a difference of 5 orders of magnitude between the two models. This is a consequence of the much higher oxygen ion escape flux which results in many more oxygen ions at higher altitudes.

For the hydrogen ions, the escape flux is independent of t_e and the density decreases with t_e, since the flow speed $w_{H^+}(s)$ will increase with t_e. This is illustrated in fig. 9 where the flow speed distribution of the hydrogen ions is plotted for different values of t_e. The flow speed of the electrons is also given in fig. 9. Since, to a first approximation, the total electron flux equals the constant hydrogen ion flux, the behaviour of the electron flow speed distribution will be the inverse of the behaviour of the electron number density distribution; i.e. if $n_e(s)$ is an increasing (or decreasing) function of t_e, then $w_e(s)$ will be a decreasing (or increasing) function of t_e. Moreover, the altitude at which two curves (e.g. $t_e = 1$ and $t_e = 2$) of the flow speed intersect

is the same as the altitude at which the corresponding curves of the number density intersect. Although the flow speed of the oxygen ions increases significantly with t_e (several orders of magnitude between the model $t_e = 0.25$ and $t_e = 4$) the values still remain very small compared to the hydrogen ion flow speed.

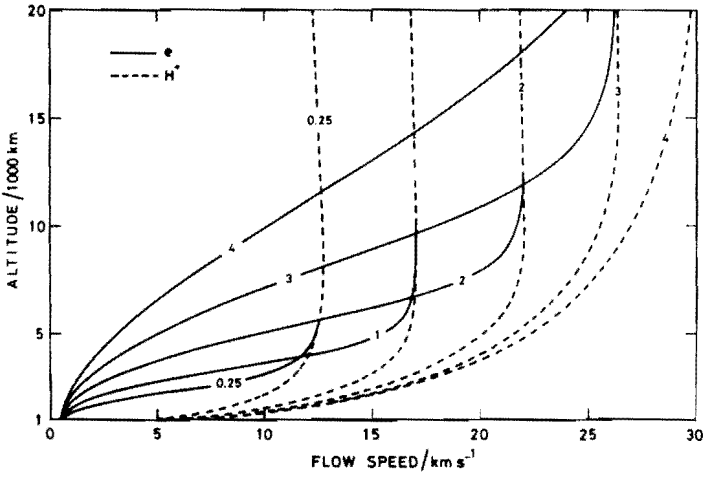

FIG. 9. — The electron and hydrogen ion flow speed in the exosphere for five different electron velocity distributions corresponding respectively to the anisotropy parameter values $t_e = 0.25$; 1; 2; 3; 4.

From the analytical formulae of the state variables summarized in Sec I we can calculate the temperature distribution by means of

$$T(s) = \frac{1}{3}[T_{\parallel}(s) + T_{\perp}(s)] \tag{58}$$

where the parallel and perpendicular temperatures are given by

$$T_{\perp}(s) = P_{\perp}(s)/kn(s) \tag{59}$$

$$T_{\parallel}(s) = [P_{\parallel}(s) - mw(s)F(s)]/kn(s). \tag{60}$$

The electron temperature and the ion temperatures are illustrated respectively in fig. 10a and 10b. For $t_e \geqq 1$ the electron temperature

in the exosphere is a monotonic decreasing function of altitude, and larger t_e-values correspond to make higher temperatures. For $t_e < 1$ the electron temperature increases rapidly just above the exobase and reaches a maximum, after which it decreases very sharply. This is illustrated in fig. 10a for the parameter value $t_e = 0.25$. A similar behaviour of the electron temperature distribution was found for the values $t_e = 0.1$; 0.5; 0.75. For $t_e = 0.9$ (not plotted in fig. 10a) the electron temperature remains almost constant between the exobase (1000 km) and 2000 km, but above this altitude $T_e(s)$ decreases.

The influence of t_e on the hydrogen and oxygen ion temperatures is much less important than on the electron temperature. Fig. 10b shows that the ion temperature distributions decrease with t_e.

4. Influence of an anisotropy in the oxygen ion velocity distribution function

Finally we will consider an (O^+, H^+, e) exosphere in which the velocity distribution of the electrons and hydrogen ions is given by a pseudo-maxwellian (i.e. $t_e = t_{H^+} = 1$ or $T_e = T_{\parallel e} = T_{\perp e}$ and $T_{H^+} = T_{\parallel H^+} = T_{\perp H^+}$) whereas the velocity distribution of the oxygen ions is a bi-maxwellian. To study the influence of t_{O^+} on the electrostatic potential at the exobase, we can proceed as in Sec. 3, since the formula for the escape flux of the oxygen ions is given by (42) (after changing the subscript e to O^+). The calculations can, however, be simplified by noting that for values of t_{O^+} which are not extremely large, the total ion flux is, for all practical purposes, given by the hydrogen flux, and therefore, to a first approximation, relation (27) reduces to

$$F_e(s_o) = F_{H^+}(s_o) \tag{61}$$

where the escape fluxes F_e and F_{H^+} are given respectively by (30) and (28) in which $t_{H^+} = 1$. The electrostatic potential at the exobase can then be determined in a self consistent way by means of condition (61) which does not contain the parameter t_{O^+}. Hence

$$\frac{d\varphi(s_o)}{dt_{O^+}} \simeq 0 \tag{62}$$

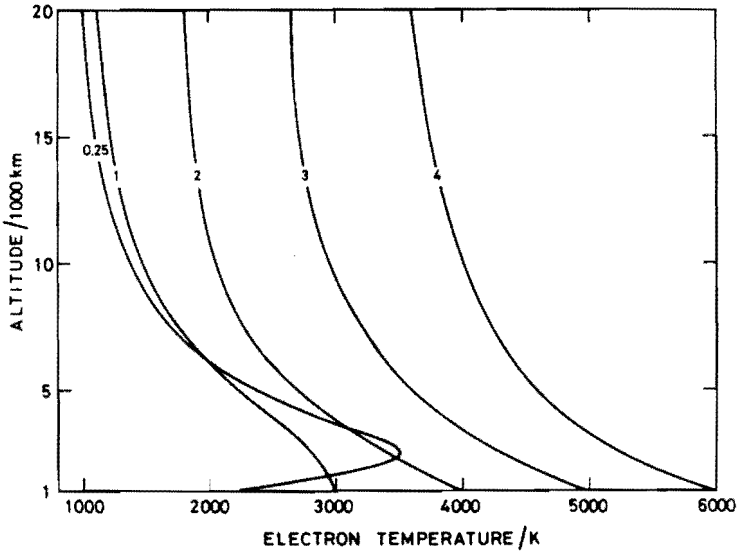

FIG. 10a. — The electron temperature distribution in the exosphere for five different electron velocity distributions corresponding respectively to the anisotropy parameter values $t_e = 0.25$; 1; 2; 3; 4.

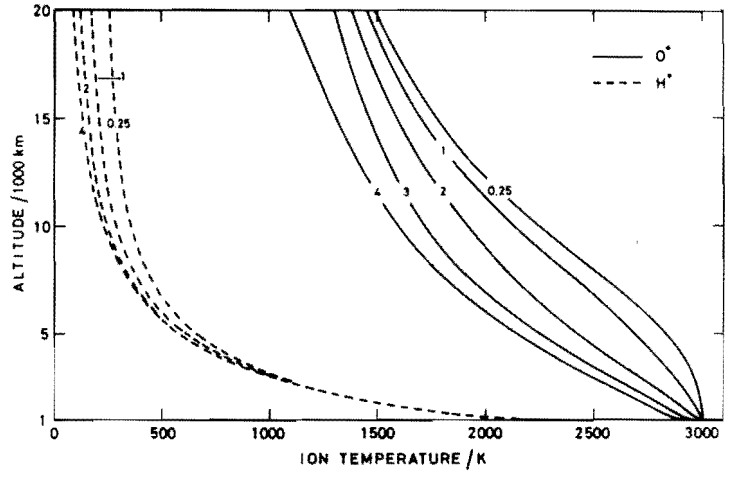

FIG. 10b. — The oxygen and hydrogen ion temperature distributions in the exosphere for five different electron velocity distributions corresponding respectively to the anisotropy parameter values $t_e = 0.25$; 1; 2; 3; 4.

and from (34) it follows that

$$t_{0+}\frac{dq_{0+}(\infty)}{dt_{0+}} = -q_{0+}(\infty) < 0 \tag{63}$$

$$\frac{dq_j(\infty)}{dt_{0+}} = 0 \tag{64}$$

where j stands for the subscripts e and H^+. This shows that $\varphi(s_o)$, the electrostatic potential at the exobase; $q_e(\infty)$, the height of the potential barrier that the escaping electrons have to overcome; and $|\, q_{H^+}(\infty)\,|$, the depth of the potential well in which the hydrogen ions move, do not vary with t_{0+}. The height of the potential barrier the escaping oxygen ions have to overcome will decrease with t_{0+}. These results are illustrated numerically by curves III in figs 1, 2a, 2b and 2c.

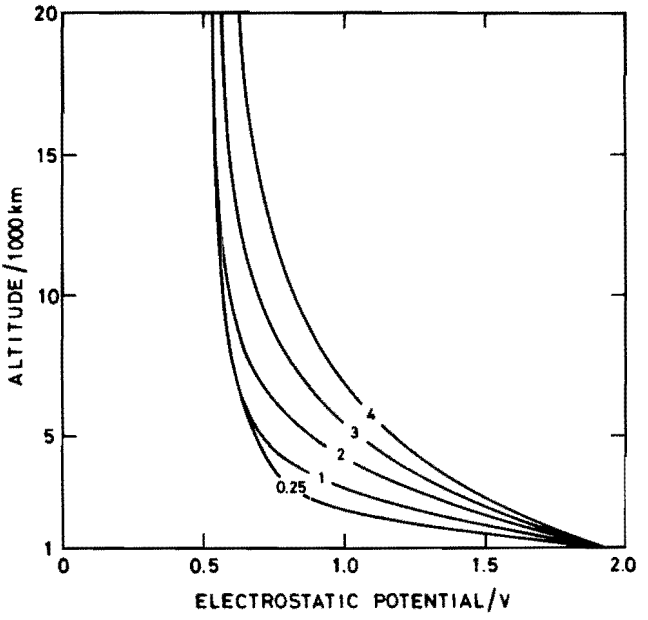

FIG. 11. — The electrostatic potential distribution in the exosphere for five different oxygen ion velocity distributions corresponding respectively to the anisotropy parameter values $t_{0+} = 0.25;\ 1;\ 2;\ 3;\ 4$.

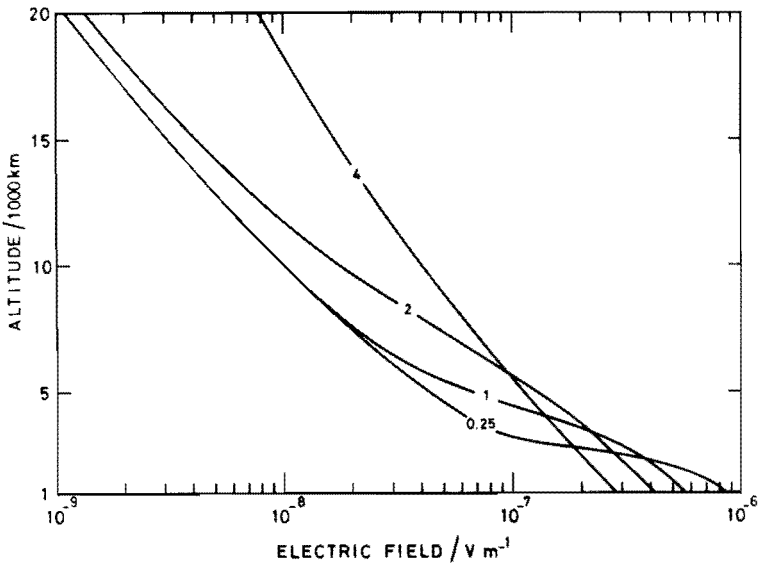

FIG. 12. — The electrostatic electric field distribution in the exosphere for four different oxygen ion velocity distributions corresponding respectively to the anisotropy parameter values $t_{O+} = 0.25; 1; 2; 4$.

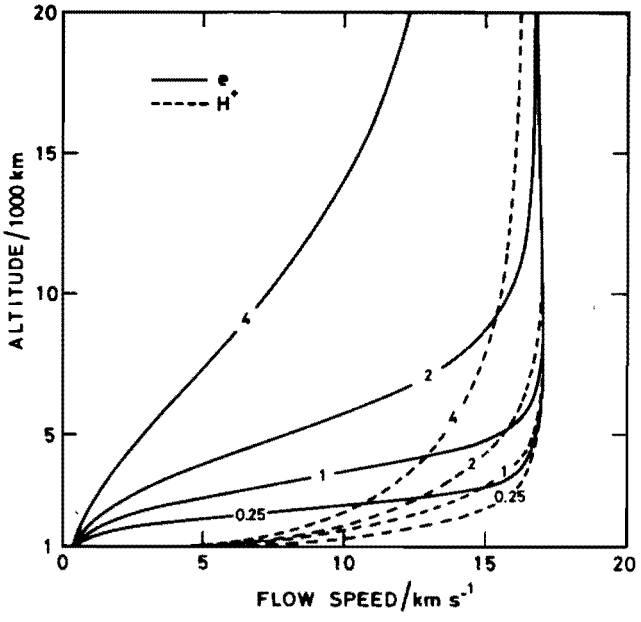

FIG. 13. — The electron and hydrogen ion flow speed in the exosphere for four different oxygen ion velocity distributions corresponding respectively to the anisotropy parameter values $t_{O+} = 0.25; 1; 2; 4$.

The electrostatic potential distribution in the exosphere shown in fig. 11 for the model calculations corresponding to the values $t_{0+} = 0.25; 1; 2; 3; 4;$ is an increasing function of t_{0+}. The electric field distributions in the exosphere are plotted in fig. 12 for $t_{0+} = 0.25; 1; 2;$ and 4. Numerical calculations have shown that, for increasing values of t_{0+}, the densities of all kinds of particles increase. On the other hand, the escape flux of the hydrogen ions and the electrons does not depend on t_{0+}, and therefore the flow speeds of the electrons and the hydrogen ions will decrease with t_{0+} as is illustrated in fig. 13.

5. Conclusions

To our knowledge, no measurements of anisotropies of the ion temperatures in the exosphere are available, and the measured anisotropic electron temperatures [Miller, 1972; Clark *et al.*, 1973] show that these values strongly depend on the geomagnetic activity and on the geomagnetic latitude. From the numerical results discussed in Sec. 2, 3 and 4, it follows that the effect of an anisotropy in the velocity distribution of each species is much more pronounced for an anisotropy in the electron velocity distribution than it is for an anisotropy in the ion velocity distributions. Reasonable values of t_e will probably never reach the extreme values 0.25 and 4 considered in the present model calculations. Therefore it can be concluded that the polar wind model in the exosphere can not be changed significantly by introducing an anisotropy in the velocity distribution at the exobase. The great advantage, however, of a polar wind model with an anisotropic velocity distribution is that the calculated proton temperature anisotropy at the exobase is no longer restricted to the constant value $1 - \frac{2}{\pi}$ as it was for the earlier kinetic model calculations [Lemaire and Scherer, 1975].

APPENDIX A

For particles moving in a potential well, as is the case for the hydrogen ions, the total number density at the exobase can be calculated

by means of formula (2) which yields

$$n(s_o) = \frac{1}{2}\mathrm{N}. \tag{A1}$$

For a given value of the number density $n(s_o)$, the parameter N can be determined easily by (A1).

For particles encountering a potential barrier, as is the case for the electrons and oxygen ions, the total number density at the exobase is given by

$$n(s_o) = n^{(\mathrm{E})}(s_o) + n^{(\mathrm{B})}(s_o) \tag{A2}$$

where the partial number densities of the escaping and ballistic particles are determined respectively by (9) and (10), and (22). Hence we obtain

$$n(s_o) = \frac{1}{2}\mathrm{N}\{1 + \mathrm{erf}(\mathrm{Q}) - \mathrm{S}(\mathrm{Q})\} \tag{A3}$$

with

$$\mathrm{Q} = [q(\infty)]^{1/2}$$

$$\mathrm{S}(\mathrm{Q}) = \begin{cases} \dfrac{1}{\kappa}\mathscr{D}(\kappa\mathrm{Q})\exp[-\mathrm{Q}^2] & \text{for } \kappa^2 \equiv t - 1 > 0 \\ \dfrac{2}{\sqrt{\pi}}\mathrm{Q}\exp[-\mathrm{Q}^2] & \text{for } t = 1 \\ \dfrac{1}{\rho}\mathrm{erf}(\rho\mathrm{Q})\exp[-t\mathrm{Q}^2] & \text{for } \rho^2 \equiv 1 - t > 0 \end{cases} \tag{A4}$$

and

$$\mathrm{erf}(z) = \frac{2}{\sqrt{\pi}}\int_0^z \exp[-x^2]dx. \tag{A5}$$

This shows that, for a given value $n(s_o)$ of the number density at the exobase, the parameter N depends on $q(\infty)$ which is proportional to the height of the potential barrier.

REFERENCES

CLARK, D. H., RAITT, W. J. and WILLMORE, A. P., 1973. A measured anisotropy in the ionospheric electron temperature, *J. Atmos. Terr. Phys.*, **35**, 63-76.

LEMAIRE, J. and SCHERER, M., 1969. Le champ électrique de polarisation dans l'exosphère ionique polaire, *Compt. Rend. Acad. Sci.* Paris, Série B, **269**, 666-669.

LEMAIRE, J. and SCHERER, M., 1970. Model of the polar ion-exosphere, *Planet. Space Sci.*, **18**, 103-120.

LEMAIRE, J. and SCHERER, M., 1971. Simple model for an ion-exosphere in an open magnetic field, *Phys. Fluids*, **14**, 1683-1694.

LEMAIRE, J. and SCHERER, M., 1972. Ion-exosphere with asymmetric velocity distribution, *Phys. Fluids*, **15**, 760-766.

LEMAIRE, J. and SCHERER, M., 1975. Contribution à l'étude des ions dans l'ionosphère polaire, *Aeronomica Acta A*-147, pp. 101.

MILLER, N. J., 1972. Possible evidence for an electron temperature anisotropy in the upper ionosphere, EOS. Trans. AGU, **53**, 472.

SCHERER, M., 1978. Open ion-exosphere with asymmetric anisotropy velocity distribution, *Bull. Acad. Sci. Belg.*, LXIV, 539-561.